Hydrothermal Effects on Isotope and Trace Element Records in Modern Reef Corals: A Study of *Porites lobata* from Tutum Bay, Ambitle Island, Papua New Guinea

THOMAS PICHLER
Department of Geology, University of South Florida, 4202 E. Fowler Ave., Tampa, FL 33620

JEFFREY M. HEIKOOP[1]
School of Geography and Geology, McMaster University, Hamilton, Ontario L8S 4M1, Canada

MICHAEL J. RISK
School of Geography and Geology, McMaster University, Hamilton, Ontario L8S 4M1, Canada

JAN VEIZER[2]
Ottawa-Carleton Geoscience Centre, University of Ottawa, Ottawa, Ontario K1N 6N5, Canada

IAIN L. CAMPBELL
Department of Physics, University of Guelph, Guelph, Ontario N1G 2W1, Canada

PALAIOS, 2000, V. 15, p. 225—234

The coral reef in Tutum Bay, Ambitle Island, Papua New Guinea, is exposed to the vigorous discharge of hydrothermal fluids (up to 98°C). This study investigates eight Porites lobata *samples that were collected throughout the area of active venting at varying distances from vent sites. A sample from a "non-hydrothermal" coral (C-29), collected 10 km north of Tutum Bay, was analyzed for comparative purposes.*

Density banding is moderately well developed in these corals and subannual bands are common. For corals from Tutum Bay, $\delta^{13}C$ ranges from −4.5 to −1.0‰ and $\delta^{18}O$ from −6.0 to −3.8‰, which are relatively depleted values for shallow water Porites. *The comparison sample, C-29, has $\delta^{13}C$ values ranging from −1.8 to −0.5‰, and $\delta^{18}O$ values of −5.4 to −4.6‰. Concentrations of As, Co, Cr, Ga, Ge, Mo, Nb, Ni, Pb, Rb, Se, W, Y and Zr were always below their respective proton probe detection limits. Ba, Br, Cu, Fe, Mn, and Zn were detected in some samples. Sr was detected in all samples and concentrations ranged from 6970 to 8240 ppm. Strontium isotope ratios of selected samples (C-5, C-8 and C-29) are very close to seawater, but Tutum Bay corals (C-5 and C-8) have lower $^{87}Sr/^{86}Sr$ values than the "non-hydrothermal" sample (C-29).*

The observed isotope patterns indicate that the hydrothermal input into Tutum Bay influences the physico-chemical conditions in the surrounding coral reef. Tutum Bay Porites lobata *show distinctly different $\delta^{13}C$ and $^{87}Sr/^{86}Sr$ records when compared to the "non-hydrothermal" sample and other corals from Papua New Guinea and elsewhere. Direct and indirect synergistic effects, including temperature, isotopic and chemical composition of vent fluids and the influence of pCO_2 on the expression of photosynthetic and kinetic stable isotope fractionation factors, are the most likely explanation for the "hydrothermal" signal seen in these corals. The $\delta^{18}O$ values are significantly correlated with the estimated amounts of hydrothermal exposure.*

0883-1351/00/0015-225/$3.00

INTRODUCTION

Previous research on sea floor hydrothermal activity has focused primarily on volcanically active portions of the mid-ocean ridges. Additional submarine hydrothermal activity can be found in much shallower water along the flanks of volcanic islands and on the tops of seamounts (e.g., Marani et al., 1997; Sedwick and Stüben, 1996). Our understanding of these shallower systems, however, is limited and only now are we starting to appreciate their importance on a larger scale. Much less is known about shallow-water venting in nearshore or shallow shelf coral-reef settings associated with volcanic islands, where substantial input of hydrothermal fluids can affect the temperature, salinity, and carbonate saturation state of ambient seawater. Every reef environment is a maze of micro-environments. Venting activity will produce very pronounced, distinctive micro-environments that have implications for paleoceanographic reconstruction from such settings.

Among coral reefs proximal to hydrothermal systems (e.g., Heikoop et al., 1996; Tomascik et al., 1996), the fringing reef around Ambitle Island, Papua New Guinea, is possibly the one subjected to the highest discharge rates of hydrothermal fluids (Pichler and Dix, 1996). Eight samples of *Porites lobata* were collected from the area of active hydrothermal venting in Tutum Bay. Isotopic and trace element measurements were performed to determine if the hydrothermal input: (1) was recorded in the chemical and isotopic composition of coral skeletons and (2) has an effect on coral metabolism. Comparable studies of organisms living near deep-sea hydrothermal vents, tracing the biolog-

[1] also: *EES-1, MS-D462, LANL, Los Alamos, NM 87545*
[2] also: *Institut für Geologie, Ruhr Universität, 44780 Bochum, Germany*

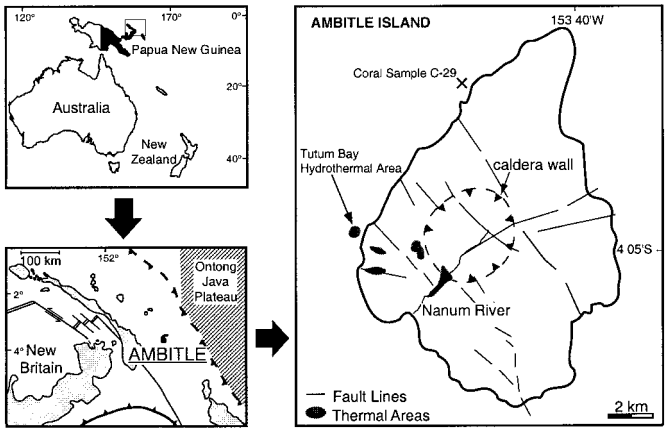

FIGURE 1—Location of Ambitle Island, one of the Feni islands in eastern Papua New Guinea (modified after Licence et al., 1987 and Pichler and Dix, 1996). Geothermal areas indicated in dark are primarily along the western side of the island. The location of sample C-29 is indicated by the X on the map to the right.

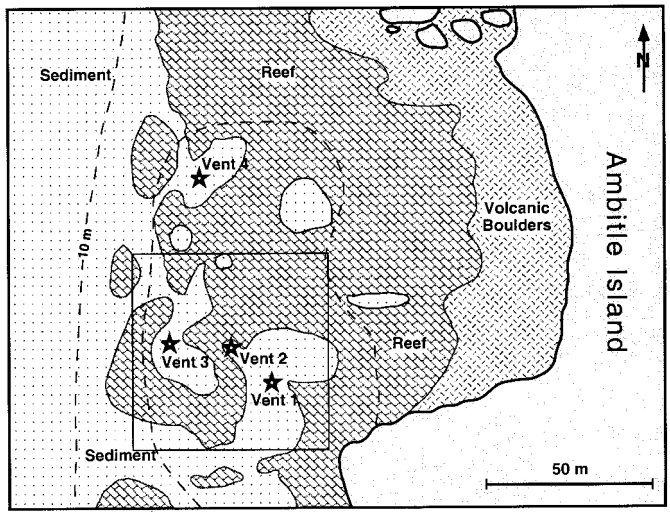

FIGURE 2—Location of hydrothermal vents within Tutum Bay on the west side of Ambitle Island. The rectangle indicates the location of the plume dispersion model in Figure 4; the dashed line indicates the extension of gaseous discharge.

ical uptake of isotopically distinct hydrothermal nutrients and the utilization of chemosynthesis as a nutritional strategy, have been reviewed, for example, by Conway et al. (1994).

LOCATION AND GEOLOGICAL SETTING

Ambitle Island is located in the southernmost of five volcanic island-groups that comprise the Tabar-Feni island-arc in eastern Papua New Guinea. The islands of the Tabar-Feni chain are Pliocene-to-Recent alkaline volcanoes that occur in the fore-arc region of the former ensimatic New Hanover-New Ireland-Bougainville island arc (Fig. 1). Ambitle is part of a Quaternary stratovolcano, characterized by a steep topography, with a central eroded caldera built on poorly exposed Oligocene marine limestone (Wallace et al., 1983). Volcanic strata (interbedded lava flows, lahar deposits, tuffs, and scoriae) dip radially from the island, presumably extending beneath the shelf. Several geothermal areas are located primarily along the western coast and in the western part of the caldera near breaches in the caldera wall (Fig. 1). Hot mud pools, springs of chloride and acid sulfate waters, and a few low-temperature fumaroles are present, with temperature and pH values ranging from 67 to 100°C and 1.9 to 9.1, respectively (Wallace et al., 1983). Except for the southern coast, where extensive freshwater input inhibits reef development, the island is surrounded completely by a fringing coral reef that extends up to several hundred meters offshore.

Tutum Bay Submarine Hot Springs

Submarine hydrothermal venting occurs at Tutum Bay (Figs. 1 and 2) in shallow (5–10 m) water along the inner shelf on which there is a patchy distribution of coral-algal reefs surrounded by medium- to coarse-grained mixed carbonate-volcaniclastic sand and gravel (Pichler and Dix, 1996). Two types of venting are present. (1) Focused discharge of a clear, two-phase fluid occurs at discrete ports, 10–15 cm in diameter, with phase separation (boiling) at the sea floor. There is no associated topographic edifice. This type of discharge produces a roaring sound underwater and has an estimated flow rate as high as 300 to 400 liters/minute (Fig. 3A). Fluid temperatures at vent orifices are between 89 and 98°C. (2) Dispersed or diffuse discharge consists of streams of gas bubbles (>95% CO_2) emerging directly through the sandy to pebbly unconsolidated sediment and through fractures in volcanic rocks (Fig. 3B). This type of venting appears to be itinerant, with shifts in locations on the order of tens of centimeters, possibly related to tortuous migration through the surface sediment. A more detailed description of Tutum Bay has been provided elsewhere (Pichler and Dix, 1996; Pichler et al., 1999) and color images can be found at http://chuma.cas.usf.edu/~pichler.

Tutum Bay hydrothermal fluids have an average $\delta^{18}O$ of −5.1‰ (VSMOW) and $\delta^{13}C$ of 1.7‰ (VPDB) and, therefore, Tutum Bay seawater may be slightly depleted in ^{18}O (0.3‰) relative to "normal" seawater (0.4‰) collected outside Tutum Bay (Pichler, 1998). Compared to seawater, the hydrothermal fluids are about 10 times less saline, but Fe, Mn, As, Cs, Tl and Si are significantly enriched (Pichler et al., 1999).

Visually, the coral reef in Tutum Bay seems to be indiscernible from its neighboring reefs to the north or south. Several bleached corals are present, but partly or wholly bleached corals are common to all reefs along the west coast of Ambitle and can be found in most reefs in the equatorial region of the western Pacific. There is no correlation between coral bleaching and distance from vent sites, and healthy corals can be found very close (<1 m) to vent orifices. The distribution of corals vs. sand is controlled by seafloor temperature, rather than by discharge of hydrothermal fluids. Sandy areas generally have a surface temperature of more than 35°C, which rapidly increases with depth. A similar phenomenon can be observed in on-land geothermal areas. In Wairakei, New Zealand, for example, the distribution and height of vege-

FIGURE 3—Underwater photographs of liquid (A) and gaseous (B) hydrothermal discharge in Tutum Bay. The field of view is ~18 m and water depth is 8 m.

tation are closely controlled by ground temperature (Burns, 1997).

SAMPLING AND ANALYTICAL METHODS

Eight *Porites lobata* samples, C-1 to C-8, were collected throughout Tutum Bay at varying distances from vent sites in April 1996. All samples were collected from depths between 6–9 m. C-29 is our "non-hydrothermal" comparison sample and was collected approximately 10 km north of Tutum Bay (Fig. 1). As such, background environmental conditions may have differed relative to Tutum Bay, irrespective of hydrothermal activity. Because of this, C-29 is included for comparative purposes only, and has not been included in any statistical analyses. C-4, C-7 and C-8 were sampled as complete coral heads and all other samples represent cores drilled (~2.5 cm diameter) along the main growth axis.

The coral slabs and cores were cut into three pieces along their growth axis. The center piece of approximately 5 mm thickness was x-rayed to obtain growth-rate information and subsequently sampled for carbon and oxygen isotope analyses. Where possible, approximately the last two years of coral growth were assessed by sampling every 1 mm of skeleton along the growth axis using a micro-drill. Samples were pretreated in areas of extreme organic contamination and taken over all skeletal elements (corallite walls, septa, etc.). Sample size was approximately 0.3 mg for all samples. In addition, corals C-5, C-8 and C-29 were sampled selectively for $^{87}Sr/^{86}Sr$ analysis. Density measurements on the last two years of coral growth were performed using a pycnometer, and calcification rates were determined as the product of density and linear extension rate.

Carbon and oxygen isotope analyses for corals were performed at McMaster University on a VG SIRA II. Precision was established using an internal coral standard and was 0.04‰ for carbon and 0.03‰ for oxygen. All results are reported in standard delta (δ) notation in per mil (‰) units, relative to the PDB standard. $^{87}Sr/^{86}Sr$ ratios were measured on a five-collector Finnigan MAT 262 solid-source mass spectrometer at the Institut für Geologie, Ruhr Universität, Bochum, following Diener et al. (1996). The average of 100 repeat measurements for the NBS 987 standard was 0.710224 ± 0.000008.

Isotopic equilibrium for Tutum Bay corals was calculated using the equations of Romanek et al. (1992) for carbon and Grossman and Ku (1986) for oxygen:

$$\delta^{13}C_{aragonite} = \delta^{13}C_{dissolved\,bicarbonate} + 2.7 \quad \text{and} \qquad (1)$$

$$T(°C) = 20.6 - 4.34(\delta_C - \delta_W). \qquad (2)$$

δ_C is the $\delta^{18}O$ of aragonite relative to PDB. No correction is made for a possible difference in ^{18}O fractionation associated with acid dissolution of aragonite (Kim and O'Neil, 1997). δ_w is reported vs. average marine water (Epstein et al., 1953), following Grossmann and Ku (1986) and T is temperature in °C. Oxygen isotope analyses of selected water samples were performed at McMaster University on a triple-collector VG OPTIMA mass spectrometer. The samples were equilibrated with CO_2 at 25°C for 1 week. The routine precision is better than 0.2‰.

Analyses of carbon-coated, polished sections were performed on the Guelph proton microprobe. Polished sections were prepared from 2-mm-thick slabs that were cut with a diamond saw from pieces directly facing the coral slab used for isotope analyses. The slabs were sonicated, extensively rinsed with de-ionized water, and impregnated with epoxy resin before being polished with aluminum powder. Any skeletal imperfections or micro-borings were clearly visible in reflected light microscopy and avoided during analyses (Allison and Tudhope, 1992).

Sample locations were chosen parallel to the growth axis, directly opposite of areas that were drilled for isotope analyses. Analyses were conducted on spots of approximately 5 μm diameter, using a 3 MeV beam and an Al filter in order to attenuate the dominant Ca peak. The instrument constant H was determined using the accurately known Sr and Fe contents of U.S. Geological Survey (USGS) BHVO-1 basalt standard, fused to a glass. Count times were 6 to 10 minutes and total element concentrations were evaluated with the GUPIX software package (Maxwell et al., 1989; 1995). In proton microprobe analyses, the LOD (limit of detection) is element specific and count rate dependent and, therefore, can change from analysis to analysis. Detection limits in ppm were: As (1.2–3.4), Ba (16.1–47.1), Br (1.2–2), Co (9.2–15.2) Cr (11.5–24.5), Cu (1.5–2.5), Fe (3.4–6.3), Ga (1.3–3.7), Ge (1.2–3.4), Mn (5.8–12.1), Mo (1.5–3.9), Nb (1.3–4), Ni (1.8–

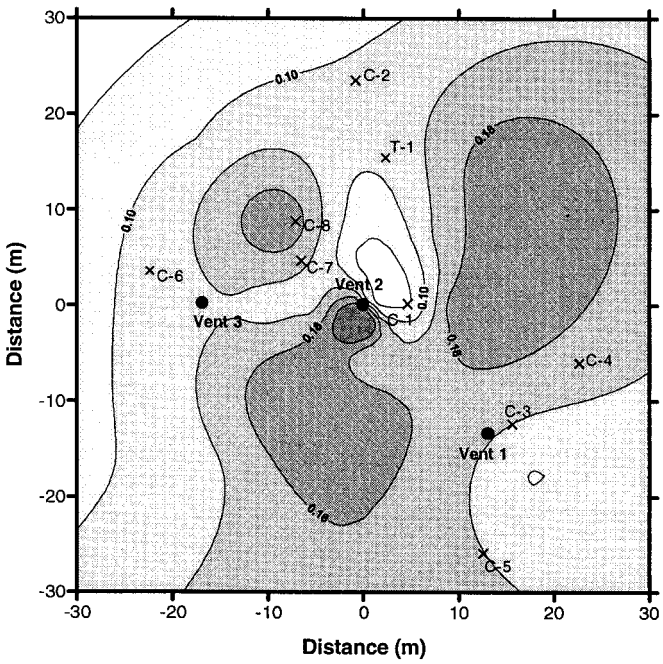

FIGURE 4—Dispersion model of hydrothermal component (HC) for the bottom water in Tutum Bay (from Pichler et al., 1999). Values for HC are in %. The darker colors indicate higher hydrothermal component. Locations where coral samples were collected are indicated (X).

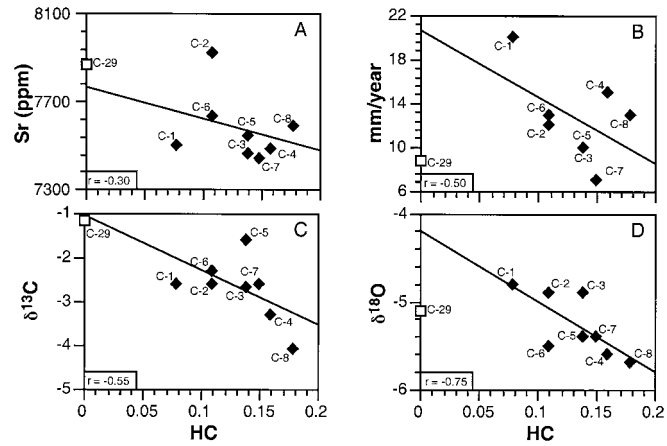

FIGURE 5—Plots of mean $\delta^{18}O$, $\delta^{13}C$, Sr concentration and growth rate vs. calculated degree of hydrothermal component (HC) in the Tutum Bay seawater. Linear regression lines are for Tutum Bay coral samples only and correlation coefficients (r) are indicated in the lower left corners.

4.3), Pb (3.9–8.7), Rb (1.3–4.3), Se (1.2–3.7), W (4.8–9.6), Y (1.4–4.6), Zn (1.3–9) and Zr (17.4–129).

RESULTS

The expected degree of hydrothermal influence on the coral samples was estimated by plotting their locations onto the map of hydrothermal plume dispersion (Fig. 4), constructed for Tutum Bay by Pichler et al. (1999). This model is based on Si as a tracer of the quantity of hydrothermal fluid present in Tutum Bay seawater. Pichler et al. (1999) selected Si, because relative to seawater, Si was approximately 500 times enriched in the vent fluids. The bottom water in Tutum Bay contains varying proportions of hydrothermal fluid and at the time of sampling, the corals were exposed to values of hydrothermal component (HC) between 0.08 and 0.18%. The model of Pichler at al. (1999), however, was constructed for waters 0.5 m above the substrate and, therefore, may seriously underestimate actual coral exposure. Nevertheless, values are a good relative measure of hydrothermal effect on Tutum Bay corals.

Coral Growth Rates

Density banding is moderately well developed in these corals and subannual bands (less distinct and often discontinuous) are common. This density pattern is likely a result of the relatively uniform equatorial climate. Growth-rate information from these corals is presented in Table 1. These growth rates are the average of the most recent two years of skeletal deposition and range from 9 to 20 mm per year. There is no significant correlation between coral growth rate and the hydrothermal input experienced by each coral (Figs. 4 and 5). A high-density band appeared to be forming at the time of collection in each of the corals. Therefore, the high-density band has

TABLE 1—Average isotopic composition, growth rate, Sr concentration, density, calcification and hydrothermal influence for Tutum Bay corals.

Coral Unit	Growth Rate mm/yr	$\delta^{13}C$[a] ‰ (PDB)	$\delta^{18}O$[a] ‰ (PDB)	$^{87}Sr/^{86}Sr$[b]	Sr ppm	Density g/cm^3	Calcification g/cm^2/yr	Hydrothermal Component %
C-1	20	−2.6 ± 0.4	−4.8 ± 0.1	n.d.	7500	1.08	2.16	0.08
C-2	12	−2.6 ± 0.4	−4.9 ± 0.2	n.d.	7900	1.25	1.50	0.11
C-3	10	−2.7 ± 0.4	−4.9 ± 0.5	n.d.	7450	1.44	1.44	0.14
C-4	15	−3.3 ± 0.3	−5.5 ± 0.2	n.d.	7490	1.27	1.90	0.16
C-5	10	−1.6 ± 0.4	−5.4 ± 0.1	0.70917	7550	1.27	1.27	0.14
C-6	13	−2.3 ± 0.3	−5.5 ± 0.1	n.d.	7650	1.35	1.75	0.11
C-7	7	−2.6 ± 0.4	−5.4 ± 0.2	n.d.	7450	1.48	1.03	0.15
C-8	13	−4.1 ± 0.3	−5.7 ± 0.2	0.70918	7590	1.11	1.45	0.18
C-29	9	−1.1 ± 0.3	−5.1 ± 0.2	0.70920	7870	1.50	1.35	n.a.

[a] Number of observations: C-1 = 27, C-2 = 27, C-3 = 20, C-4 = 27, C-5 = 2, C-6 = 27, C-7 = 11, C-8 = 27 and C-29 = 27.

[b] Number of observations and standard error is given in Table 2; n.d. = not determined; n.a. = not applicable.

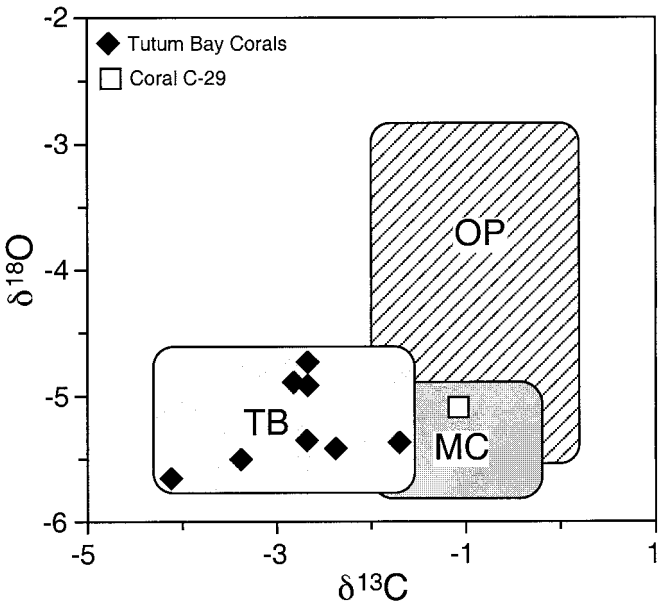

FIGURE 6—$\delta^{18}O$ and $\delta^{13}C$ values of Tutum Bay coral skeletons compared to other corals from Papua New Guinea and elsewhere. TB: Tutum Bay corals (C-1 to C-8), MC: A 69- year record for a *Porites* from Madang (Tudhope et al., 1995), at approximately the same latitude as Tutum Bay, but 1000 km to the west; OP: *Porites* from other modern coral reefs (Aharon, 1991 and references therein).

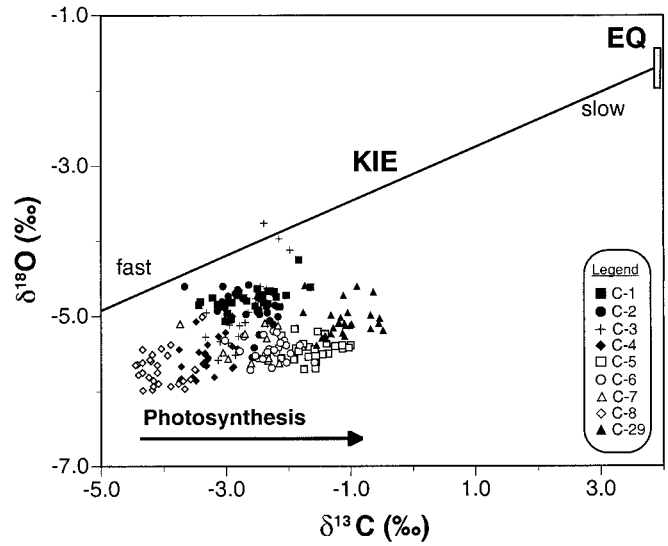

FIGURE 7—$\delta^{18}O$ vs. $\delta^{13}C$ of Tutum Bay (C-1 to C-8) and reference (C-29) corals. Note that several corals plot as nearly distinct fields (for statistical significance see Appendix 1). Isotopic equilibrium has been calculated using equations given in the text. $\delta^{18}O$ of the water mass has been taken as 0.45‰. The range in oxygen isotopic equilibrium represents a possible temperature range in Tutum Bay. The range in carbon isotopic equilibrium values represents a possible range in $\delta^{13}C$ of DIC. The upper value is calculated from a measured open ocean seawater DIC value of 1.2‰. Assuming a small contribution of hydrothermal fluids ($\delta^{13}C$ of −1.8‰; Pichler, 1998), $\delta^{13}C$ equilibrium should be between 3.8 and 3.9‰. Possible causes of isotopic variation are: (1) variations in isotopic equilibrium (field marked EQ); (2) coral growth rate (isotopic variation will occur along the trend delineating kinetic isotope effects, KIE); and (3) differential ^{13}C enrichments related to the degree of photosynthesis. Note that most samples plot to the right of the kinetic isotope effect line, suggesting net autotrophy. Compare to figure 13 in McConnaughey (1989).

been used as a chronological marker, representing the month of April, when interpreting isotopic records (Fig. 6).

Density and calcification data (averages of the last two years of growth) for these corals also are provided in Table 1. Density and growth rate are correlated inversely ($r = -0.79$, $p = 0.019$, $n = 8$), whereas neither density nor calcification rate show significant trends with hydrothermal input. Of all the growth parameters, calcification rate shows the strongest trend with hydrothermal input ($r = -0.53$, $p = 0.18$).

Isotopes

Oxygen and carbon isotope data are presented graphically in Figures 6, 7 and 8. Data summaries are provided in Table 1. $\delta^{13}C$ ranges from −4.5 to −1.0‰ and $\delta^{18}O$ from −6.0 to −3.8‰ for corals from Tutum Bay. The "non-hydrothermal" sample, C-29, has $\delta^{13}C$ values ranging from −1.8 to −0.5‰, and $\delta^{18}O$ values of −5.4 to −4.6‰. The $\delta^{18}O$ values for this specimen are within the range of Tutum Bay corals. However, $\delta^{13}C$ is generally higher and closer to values for *Porites* from "non-hydrothermal" areas (Fig. 6). In $\delta^{18}O$ vs. $\delta^{13}C$ space, it can be seen that many of these corals plot as nearly distinct fields, representing distinct isotopic signatures (Fig. 7). There is a significant positive correlation between $\delta^{13}C$ and $\delta^{18}O$ for the eight hydrothermally affected corals ($r = 0.31$, $p < 0.01$).

Selected examples of isotopic measurements versus distance into the skeleton are shown in Figure 8. C-8 represents a coral that received high amounts of hydrothermal input compared to other samples (Fig. 4); C-3 represents a coral growing immediately adjacent to Vent 1, which has the highest hydrothermal discharge (although the benthic waters surrounding this coral have relatively low hydrothermal content); and C-29 displays isotopic data for our comparison sample. There is only weak evidence of clear annual cyclicity in these corals. $\delta^{18}O$ generally shows an annual range of approximately 0.5‰ and $\delta^{13}C$ varies by about 1‰ in each sample.

No significant correlation exists between any of the growth parameters (growth rate, density, calcification rate) and either mean $\delta^{18}O$ or mean $\delta^{13}C$ for the eight hydrothermal corals sampled. A significant inverse correlation occurs, however, between $\delta^{18}O$ and the degree of hydrothermal component ($r = -0.75$, $p < 0.05$, $n = 8$; Fig. 5). Average $\delta^{13}C$ values of Tutum Bay corals show only a very weak inverse relationship with hydrothermal input ($r = -0.55$, $p = 0.16$, $n = 8$; Fig. 5). No significant relationship exists between mean Sr content and hydrothermal component (Fig. 5).

Subsamples of corals C-29, C5 and C8 that showed either relatively high or low $\delta^{18}O$ and $\delta^{13}C$ values were analyzed for $^{87}Sr/^{86}Sr$. Results for these samples are provided in Table 2 and graphically displayed in Figure 9. Ratios range from 0.70914 to 0.70924 and are very close to the values for local seawater 0.70918 ± 0.000008 (Pichler et al., 1999). When compared to the "non-hydrothermal" coral (C-29), both samples from Tutum Bay (C-5 and C-8) show a significantly lower $^{87}Sr/^{86}Sr$ (Fig. 9).

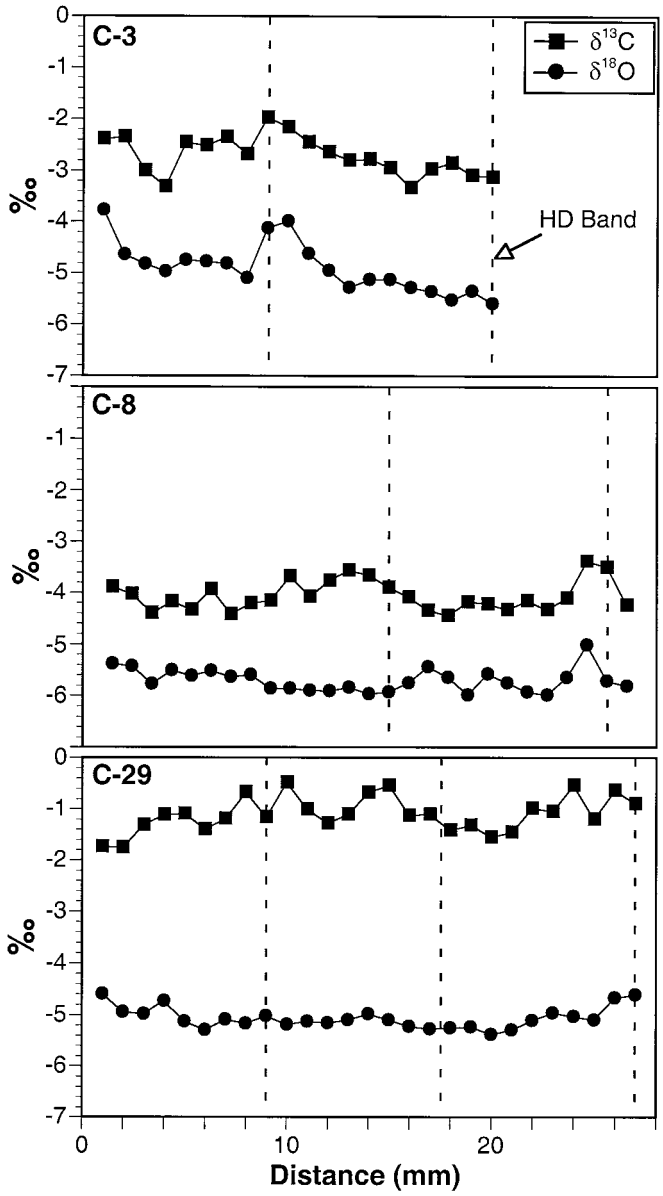

FIGURE 8—$\delta^{18}O$ and $\delta^{13}C$ values of coral skeletons C-3, C-8, and C-29 (''non-hydrothermal'' coral) versus distance from the top of the corallum. Locations of high density bands are indicated (dashed line). The top of the skeleton and each high-density band represent primary skeletal deposition during the month of April. The distance between the top of the skeleton and each subsequent high-density band, therefore, represents one year of skeletal deposition.

Trace Elements

At standard experimental conditions, most elements ($Z > 22$) were below their respective detection limit given acceptable counting times of approximately 10 minutes. Concentrations of As, Co, Cr, Ga, Ge, Mo, Nb, Ni, Pb, Rb, Se, W, Y and Zr were always below their respective detection limits. Ba, Br, Cu, Fe, Mn, and Zn were detected in some samples, but due to their scarcity, element-to-element correlation was impractical. Sr was detected in all samples and its concentration ranged from 6970 to 8240 ppm with a mean of 7640 ppm ($n = 53$, $\sigma = 239$). No significant correlation exists between any of the growth parameters (growth rate, density, calcification rate) and mean Sr for the eight hydrothermal corals sampled (Fig. 5). The Sr concentration in our comparison sample (C-29) is higher than those for Tutum Bay corals with the exception of C-2 (Table 1 and Appendix 1). Based on their Sr content, Tutum Bay corals do not fall into distinct groups, as observed for $\delta^{13}C$ and $\delta^{18}O$ (Appendix 1).

TABLE 2—Carbon, oxygen and strontium isotopic compositions for selected Tutum Bay corals.

Sample	Point (mm)	$\delta^{13}C$ (‰)	$\delta^{18}O$ (‰)	$^{87}Sr/^{86}Sr$	± 2 Standard Error
C-5	1	−2.1	−5.3	0.70914	0.000009
	13	−1.0	−5.4	0.70916	0.000010
	19	−1.5	−5.5	0.70918	0.000008
	24	−2.4	−5.5	0.70919	0.000013
C-8	1	−3.9	−5.4	0.70914	0.000009
	18	−4.5	−5.6	0.70915	0.000006
	23	−4.3	−6.0	0.70921	0.000010
	25	−3.4	−5.0	0.70921	0.000009
C-29	1	−1.7	−4.6	0.70921	0.000008
	6	−1.4	−5.3	0.70924	0.000009
	26	−0.6	−4.7	0.70919	0.000013

DISCUSSION

There is no clear effect of hydrothermal fluids on coral growth rate measurements in Tutum Bay. Whereas annual temperature and insolation cycles are thought to affect density-band formation and annual growth rate, common growth and density patterns may be lacking even between corals within a single reef in which climatic variables are relatively uniform (Lough and Barnes, 1992). Given this natural tendency towards variation in growth parameters within relatively homogeneous environments, it is unlikely that clear relationships would be found with-

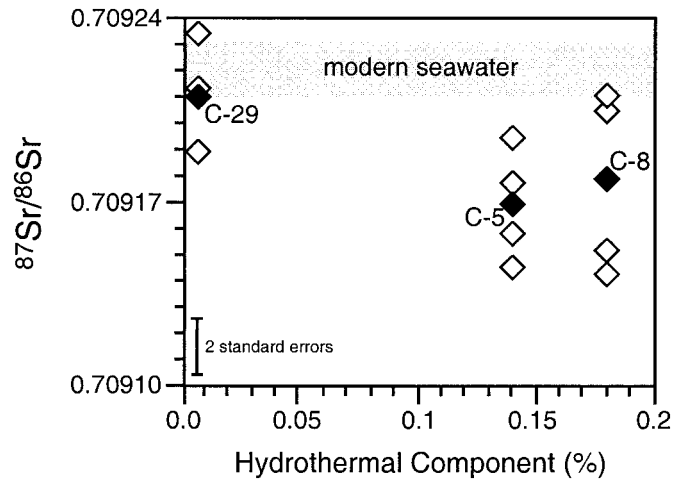

FIGURE 9—$^{87}Sr/^{86}Sr$ vs. calculated degree of hydrothermal component (HC) for samples C-29, C-5 and C-8. The shaded areas represent the value for $^{87}Sr/^{86}Sr$ of modern seawater (Veizer and Compston, 1974; Burke et al., 1982). Open diamonds represent measured values and solid diamonds indicate their respective arithmetic means.

in the very heterogeneous system studied here. The weak inverse trend between calcification rate and hydrothermal input may be symptomatic of some degree of coral stress.

Considering that the measured effect of hydrothermal fluids on Tutum Bay corals is small (<0.2% HC), it is not surprising that we did not detect As, Co, Cr, Ga, Ge, Mo, Nb, Ni, Pb, Rb, Se, W, Y or Zr during proton probe analyses. Aragonite preferentially incorporates cations larger than Ca (Sr, Na, Ba, U), while calcite favors the smaller Mg, Fe, Mn, Zn, and Cd. Distribution coefficients, however, are generally low (Veizer, 1983). Given the limited number of observations, it is not possible to relate the slightly elevated concentrations of Cu, Mn and Fe in some corals to the hydrothermal input. Strontium, although detected in all samples, is a poor indicator of hydrothermal activity in Tutum Bay. This is because its concentration in seawater and hydrothermal fluid is essentially the same (Pichler et al., 1999), and the water temperature in the bay is too invariable to cause a distribution coefficient driven variation in Sr concentrations (e.g., Beck et al., 1992).

The lack of annual cyclicity in the isotope data (Fig. 8) possibly reflects buffering of temperature and $\delta^{18}O$ of bay waters by a combination of constant hydrothermal input and a relatively uniform equatorial climate. Annual temperature variations are only on the order of 2.5°C. This temperature range is matched by the observed annual $\delta^{18}O$ variation in Tutum Bay corals, assuming a temperature dependence of approximately −0.22°C per 1‰ (Carriquiry et al., 1994). Intra- and interannual $\delta^{18}O$ variations in other Papua New Guinea corals have been attributed to variations in the input of ^{18}O-depleted rainfall (Aharon, 1991; Tudhope et al., 1995). Rainfall at this site has a $\delta^{18}O$ value of approximately −5‰ (Pichler and Dix, 1996). This may be sufficiently low relative to seawater to account for some of the observed coral $\delta^{18}O$ variation.

Of greater interest, however, are the distinct isotopic signatures of many of the corals and their correlation with the degree of hydrothermal influence. The $\delta^{18}O$ values for the Tutum Bay corals are within the measured range for shallow water (<10 m) members of the genus *Porites* (e.g., Aharon, 1991; Allison et al., 1996). Corals with $\delta^{18}O$ values similar or even lower than those of Tutum Bay corals tend to grow in areas with high sea-surface temperatures or abundant input of ^{18}O-depleted rainfall or flood waters (e.g., Gagan et al., 1994; Wellington and Dunbar, 1995).

The $\delta^{13}C$ values of Tutum Bay corals are among the lowest when compared to records from other studies. Only corals experiencing thermal stress or greatly reduced light availability (photosynthesis) have values as low as those seen in coral C-8 (e.g., Allison et al., 1996; Gagan et al., 1994). Generally, $\delta^{13}C$ values of corals affected by vent fluids are distinctly lower than those of *Porites* from other locations in Papua New Guinea and elsewhere (Fig. 6). Considering Tutum Bay corals were collected in a restricted area from approximately the same depth, the range in isotopic values is large. The fact that some corals plot as distinct fields also is interesting and likely reflects the heterogeneous environment created by the hydrothermal venting.

The main potential sources of variation in both $\delta^{18}O$ and $\delta^{13}C$ are shown in Figure 7. These include variations in environmental conditions (temperature and the chemical and isotopic composition of the water), which would affect isotopic equilibrium, kinetic isotope effects related to growth parameters, and metabolic effects including photosynthetic ^{13}C enrichment of the internal dissolved inorganic carbon (DIC) pool. The strong depletion in ^{18}O and ^{13}C seen in the most strongly vent-affected corals is likely a combination of factors, all acting to perturb the isotopic signals in the same direction.

Theoretically, increased temperature associated with venting could lead to lower $\delta^{18}O$ of vent corals, but is unlikely to directly affect coral skeletal $\delta^{13}C$ (see equation [1]). The small amounts of hydrothermal input measured at 0.5 m above the substrate, however, will have a negligible affect on seawater temperature. While providing a measure of relative exposure of corals to hydrothermal fluids, these calculated hydrothermal components may underestimate exposure nearer to the sediment-water interface, where temperatures may be higher as a result of diffuse discharge and radiant heat from the substrate.

The isotopic composition of the vent fluids also could lead to isotopically depleted coral carbonate. Vent waters have $\delta^{18}O$ of ~ -5‰ and $\delta^{13}C_{DIC}$ of ~ -1.7‰. Both of these values are slightly depleted relative to average seawater. The overall lack of variation in $\delta^{18}O$ of the water mass at 0.5 m above the substrate suggests that any such effects will be small, although they might be larger for smaller corals growing closer to the substrate. The hydrothermal gases that discharge throughout the bay are composed of >95% CO_2 and have a $\delta^{13}C$ of −2.5‰. Their influence on the $\delta^{13}C$ of Tutum Bay corals is not accounted for by the plume dispersion model. The greater availability of ^{12}C and an increased pCO_2 may significantly affect the coral isotope record.

Kinetic isotope effects occurring during the hydration and hydroxylation of CO_2 during calcification can lead to simultaneous decreases in both $\delta^{13}C$ and $\delta^{18}O$ values of coral skeletons. Lower values are usually associated with faster growth, lower density and higher calcification rates (McConnaughey, 1989; Allison et al., 1996; Cohen and Hart, 1997). The overall positive correlation between $\delta^{13}C$ and $\delta^{18}O$ for all subsamples of corals C1 to C8, and the general trend of the data towards isotopic equilibrium could be taken as evidence for strong kinetic isotope effects (e.g., Heikoop, 1997). Tutum Bay corals, however, show no relationship between growth parameters and isotopic composition. It is possible that the most vent affected corals display greater than average kinetic isotope effects as a result of some other physico-chemical factor associated with venting that has not been recognized previously. The discharge of hydrothermal gas also could be a factor in the degree of expression of kinetic isotope effects. Precipitation of ^{13}C-depleted carbon in the skeleton leads to isotopic enrichment of the coral internal DIC pool and skeletal kinetic isotope depletion occurs relative to this enriched pool (see fig. 8 in McConnaughey et al., 1997). Under conditions of high environmental pCO_2, however, less enrichment of this internal DIC pool will occur and the carbon kinetic isotope effects will be more fully expressed. Similar effects also may affect $\delta^{18}O$.

If the corals were stressed photosynthetically by the hydrothermal inputs to the bay, reduced photosynthesis could lead to lower $\delta^{13}C$ of coral skeletons (Fig. 7). Thermal stress can lead to decreased ratios of photosynthesis to

respiration in corals and, hence, to lower skeletal $\delta^{13}C$ (Swart, 1983; Carriquiry et al., 1994). We have little evidence, however, that the most vent-affected corals are stressed, aside from slightly lower calcification rates. Growth rates are relatively high, and no bleaching was observed in these corals. The corals in this study mostly plot to the right of the kinetic isotope line, and corals that plot in this area have been interpreted as net autotrophs (e.g.,McConnaughey, 1989; Heikoop, 1997). Thermal stress seems to have an impact on the distribution of corals in the bay (i.e., coral cover vs. sand cover), but perhaps where corals are able to establish themselves on the substrate, they are able to maintain high levels of photosynthesis due to the presence of increased pCO_2 in the water column that will tend to increase photosynthetic efficiency.

Increased pCO_2 in waters surrounding the most vent-affected corals also could affect the degree of expression of photosynthetic enrichment of the internal DIC pool. With more CO_2 available, the isotopic composition of the pool will be harder to perturb and coral skeletons will tend to be depleted (less enriched by photosynthesis) in ^{13}C.

All of the effects described above will act in the same direction, resulting in a depletion of skeletal ^{13}C and ^{18}O for the most vent-affected corals. The multitude of biological and inorganic factors make it difficult to detect the direct cause of vent-related isotope signatures. It is possible, however, that vent chemistry (e.g., CO_2 concentrations) is as important or even more important than temperature. A combination of vent-related effects, however, appears to be large enough to affect coral $\delta^{13}C$ and $\delta^{18}O$ despite the low hydrothermal contribution to bay waters.

Unlike the light stable isotopes, Sr isotopes are generally not affected by biological and/or inorganic fractionation, because the mass difference between the ^{87}Sr and ^{86}Sr is only 1.2 %. This difference is too small to cause a measurable fractionation during precipitation of calcium carbonate. As a result, the $^{87}Sr/^{86}Sr$ in marine carbonates is controlled entirely by its ratio in seawater. The vent fluids have a significantly lower $^{87}Sr/^{86}Sr$ (Pichler, 1998) than average modern seawater (Veizer and Compston, 1974; Burke et al., 1982) and, therefore, Tutum Bay seawater has to be slightly depleted in ^{87}Sr. This depletion is evident in the $^{87}Sr/^{86}Sr$ of coral skeletons of the samples from Tutum Bay when compared to the "non-hydrothermal" coral and modern seawater (Fig. 9). The lower $^{87}Sr/^{86}Sr$ of Tutum Bay corals must be directly related to the lower $^{87}Sr/^{86}Sr$ of Tutum Bay seawater, which, in turn, is related to the hydrothermal system. As a result, the $^{87}Sr/^{86}Sr$ ratios in Tutum Bay corals are a good indication of the hydrothermal influence experienced by Tutum Bay corals.

SUMMARY AND CONCLUSIONS

Hydrothermal activity in Tutum Bay has a discernible impact on the chemistry of reef coral skeletons. The $\delta^{18}O$, $\delta^{13}C$ and $^{87}Sr/^{86}Sr$ values of a coral skeleton seem to be sensitive recorders of small amounts of hydrothermal fluid input. Tutum Bay *Porites lobata* show distinctly different $\delta^{13}C$ when compared to a "non-hydrothermal" sample from Ambitle island and to literature-derived data for other corals from Papua New Guinea and elsewhere. Similarly, $^{87}Sr/^{86}Sr$ values are lower in vent-affected corals relative to the "non-hydrothermal" sample. The vent-affected corals also show significant correlation between $\delta^{18}O$ and hydrothermal component (HC). Those corals exposed to the highest hydrothermal influence show the lowest $\delta^{18}O$ and $\delta^{13}C$. $\delta^{18}O$ and $\delta^{13}C$ may show a larger response to hydrothermal venting than $^{87}Sr/^{86}Sr$ or trace element signatures because, in addition to the direct effects of the hydrothermal fluids, the presence of abundant vent CO_2 can influence the degree of isotopic fractionation. Vent CO_2 will have no impact on Sr isotopes and trace element signatures.

The hydrothermal system most likely affects the isotope records of Tutum Bay corals in two ways: (1) directly by changing the physico-chemical conditions of aragonite precipitation (i.e., fluid mixing, increased temperature) and (2) indirectly by affecting the degree of expression of various kinetic isotope effects (KIE) and metabolic fractionation factors. Factors such as thermal or photosynthetic stress may be of secondary importance. Elevated pCO_2 may be a factor in reducing bleaching in such a stressful environment. Future work in this area will examine the relative importance of the various factors.

Even small amounts of hydrothermal venting can perturb environmental conditions sufficiently to affect coral skeletal chemistry. Therefore, areas where venting is confirmed or suspected should be avoided when trying to reconstruct regional climate signals based, for example, on oxygen isotope paleothermometry. The hydrothermal signals we have identified here could potentially be used to help identify the presence of venting activity in older reef environments. However, given the small magnitude of the $^{87}Sr/^{86}Sr$ signal and the fact that other factors could cause strong depletion in ^{13}C and ^{18}O, it would be necessary to combine this information with other indicators of hydrothermal activity such as the presence of hydrothermal iron and calcite precipitates.

ACKNOWLEDGMENTS

Most of this research was funded by an American Chemical Society, Petroleum Research Grant (No. 31585-AC8) to Jan Veizer. Isotope analyses at McMaster University were supported through a NSERC grant to Michael Risk. Thomas Pichler acknowledges the support of two Geological Society of America Student Research Grants (No. 5681-95 and 5904-96). We all would like to thank Ines Guerrero, George Mazarek, Martin Knyf, and Dieter Buhl for coral preparation and isotope analyses, and Bill Teesdale for help during proton probe analyses. Ted McConnaughey read an earlier version of this manuscript and provided excellent suggestions for its improvement. Thomas Pichler is very grateful to Donna Switzer for her help underwater.

REFERENCES

AHARON, P., 1991, Recorders of reef environment histories: Stable isotopes in corals, giant clams, and calcareous algae: Coral Reefs, v. 10, p. 71–90.

ALLISON, N., and TUDHOPE, A.W., 1992, Nature and significance of geochemical variations in coral skeletons as determined by ion microprobe analysis, Seventh International Coral Reef Symposium: University of Guam Marine Laboratory, Guam, p. 173–178.

ALLISON, W., TUDHOPE, A.W., and FALLICK, A.E., 1996, Factors influ-

encing the stable carbon and oxygen isotopic composition of *Porites lutea* coral skeletons from Phuket, South Thailand: Coral Reefs, v. 15, p. 43–57.

BECK, W.J., EDWARDS, R.L., TAYLOR, F.W., RECY, J., ROUGERIE, F., JOANNOT, P., and HENIN, C., 1992, Sea-surface temperature from coral skeletal strontium/calcium ratios: Science, v. 257, p. 644–646.

BURKE, W.H., DENISON, R.E., HETHERINGTON, E.A., KOEPNICK, R.B., NELSON, N.F., and OTTO, J.B., 1982, Variation of seawater $^{87}Sr/^{86}Sr$ throughout Phanerozoic time: Geology, v. 10, p. 516–519.

BURNS, B., 1997, Vegetation change along a geothermal stress gradient at the Te Kopia steam field: Journal of the Royal Society of New Zealand, v. 27, p. 279–294.

CARRIQUIRY, J.D., RISK, M.J., and SCHWARCZ, H.P., 1994, Stable isotope geochemistry of corals from Costa Rica as proxy indicator of the El Niño/Southern Oscillation (ENSO): Geochimica Cosmochimica Acta, v. 58, p. 335–351.

COHEN, A.L., and HART, S.R., 1997, The effect of colony topography on climate signals in coral skeletons: Geochimica Cosmochimica Acta, v. 61, p. 3905–3912.

CONWAY, N.M., KENNICUTT II, M.C., and VAN DOVER, C.L., 1994, Stable isotopes in the study of marine chemosynthetic-based ecosystems: *in* Lajtha, K., and Michener, R.H., eds., Stable Isotopes in Ecology and Environmental Science: Blackwell Scientific Publications, London, p. 158–186.

DIENER, A., EBNETH, S., VEIZER, J., and BUHL, D., 1996, Strontium isotope stratigraphy of the Middle Devonian: Brachiopods and conodonts: Geochimica Cosmochimica Acta, v. 60, p. 639–652.

EPSTEIN, S., BUCHSBAUM, R., LOWENSTAM, H.A., and UREY, H.C., 1953, Revised carbonate-water isotopic temperature scale: Geological Society of America Bullettin, v. 64, p. 1315–1326.

GAGAN, M.K., CHIVAS, A.R., and ISDALE, P.J., 1994, High-resolution records from corals using temperature and mass-spawning chronometers: Earth and Planetary Science Letters, v. 121, p. 549–558.

GROSSMAN, E.L., and KU, T.-L., 1986, Oxygen and carbon isotope fractionation in biogenic aragonite: Temperature effects: Chemical Geology, v. 59, p. 59–74.

HEIKOOP, J.M., 1997, Environmental Signals in Coral Tissue and Skeleton: Examples from the Caribbean and Indo-Pacific: Unpublished Ph.D. Thesis, McMaster University, Hamilton, 166 p.

HEIKOOP, J.M., TSUJITA, C.J., RISK, M.J., and TOMASCIK, T., 1996, Corals as proxy recorders of volcanic activity: Evidence from Banda Api, Indonesia: PALAIOS, v. 11, p. 286–292.

KIM, S.-T., and O'NEIL, J.R., 1997, Equilbrium and nonequilibrium oxygen isotope effects in synthetic carbonates: Geochimica Cosmochimica Acta, v. 61, p. 3461–3475.

LICENCE, P.S., TERRILL, J.E., and FERGUSSON, L.J., 1987, Epithermal gold mineralization, Ambitle Island, Papua New Guinea, Pacific Rim Congress 87: Gold Coast, Queensland, Australasian Institute of Mining and Metallurgy, p. 273–278.

LOUGH, J.M., and BARNES, D.J., 1992, Comparisons of skeletal density variations in *Porites* from the central Great Barrier Reef: Journal of Experimental Marine Biology and Ecology, v. 155, p. 1–25.

MARANI, M.P., GAMBERI, F., and SAVELLI, C., 1997, Shallow-water polymetallic sulfide deposits in the Aeolian island arc: Geology, v. 25, p. 815–818.

MAXWELL, J.A., TEESDALE, W.J., and CAMPBELL, J.L., 1989, The Guelph PIXE software package: Nuclear Instruments and Methods in Physics Research, v. B43, p. 218–230.

MAXWELL, J.A., TEESDALE, W.J., and CAMPBELL, J.L., 1995, The Guelph PIXE software package II: Nuclear Instruments and Methods in Physics Research, v. B95, p. 407–421.

MCCONNAUGHEY, T., 1989, ^{13}C and ^{18}O isotopic disequilibrium in biological carbonates: II. In vitro simulation of kinetic isotope effects: Geochimica Cosmochimica Acta, v. 53, p. 163–171.

MCCONNAUGHEY, T.A., BURDETT, J., WHELAN, J.F., and PAULL, C.K., 1997, Carbon isotopes in biological carbonates: Respiration and photosynthesis: Geochimica Cosmochimica Acta, v. 61, p. 611–622.

PICHLER, T., 1998, Shallow-water hydrothermal activity in a coral-reef ecosystem, Ambitle Island, Papua New Guinea: Unpublished Ph.D. Thesis, Univerity of Ottawa, Ottawa, 206 p.

PICHLER, T., and DIX, G.R., 1996, Hydrothermal venting within a coral reef ecosystem, Ambitle Island, Papua New Guinea: Geology, v. 20, p. 435–438.

PICHLER, T., VEIZER, J., and HALL, G.E.M., 1999, The chemical composition of shallow-water hydrothermal fluids in Tutum Bay, Ambitle Island, Papua New Guinea and their effect on ambient seawater: Marine Chemistry, v. 64, p. 229–252.

ROMANEK, C.S., GROSSMAN, E.L., and MORSE, J.W., 1992, Carbon isotopic fractionation in synthetic aragonite and calcite: Effects of temperature and precipitation rate: Geochimica et Cosmochimica Acta, v. 56, p. 419–430.

SEDWICK, P., and STÜBEN, D., 1996, Chemistry of shallow submarine warm springs in an arc-volcanic setting: Vulcano Island, Aeolian Archipelago, Italy: Marine Chemistry, v. 53, p. 146–161.

SWART, P.K., 1983, Carbon and oxygen isotope fractionation in scleractinian corals: A review: Earth Science Reviews, v. 19, p. 51–80.

TOMASCIK, T., VAN WOESIK, R., and MAH, A.J., 1996, Rapid recolonization of a recent lava flow following a volcanic eruption, Banda Islands, Indonesia: Coral Reefs, v. 15, p. 169–175.

TUDHOPE, A.W., SHIMMIELD, G.B., CHILCOTT, C.P., JEBB, M., FALLICK, A.E., and DALGLEISH, A.N., 1995, Recent changes in the far western equatorial Pacific and their relationship to the Southern Oscillation: Oxygen isotope records from massive corals, Papua New Guinea: Earth and Planetary Science Letters, v. 136, p. 575–590.

VEIZER, J., 1983, Chemical diagenesis of carbonate rocks: Theory and application of trace element technique: *in* Arthur, M.A., and Anderson, T.F., eds., Stable Isotopes in Sedimentary Geology: Society of Economic Paleontologists and Mineralogists, Short Course No. 10, p. 3.1–3.100.

VEIZER, J., and COMPSTON, W., 1974, $^{87}Sr/^{86}Sr$ compostion of seawater during the Phanerozoic: Geochimica et Cosmochimica Acta, v. 38, p. 1461–1484.

WALLACE, D.A., JOHNSON, R.W., CHAPPELL, B.W., ARCULUS, R.J., PERFIT, M.R., and CRICK, I.H., 1983, Cainozoic volcanism of the Tabar, Lihir, Tanga, and Feni islands, Papua New Guinea: Geology, whole-rock analyses, and rock-forming mineral compositions: Bureau of Mineral Resources Geology and Geophysics, Sydney, 66 p.

WELLINGTON, G.M., and DUNBAR, R.B., 1995, Stable isotopic signature of El Nino-Southern Oscillation events in eastern tropical Pacific reef corals: Coral Reefs, v. 14, p. 5–25.

ACCEPTED FEBRUARY 2, 2000

APPENDIX 1

Means comparison for $\delta^{13}C$, $\delta^{18}O$ and Sr analyzed in corals from Ambitle Island. Column A shows the distribution of values for each sample. The dashed line across the middle is the grand mean. The top and bottom of the diamonds indicate the 95% confidence interval and the line through the middle of a diamond indicates the mean. In order to account for the imbalance in the data set (i.e., the means do not all have the same number of observations), we plotted comparison circles in columns B and C. The radius of a circle is the 95% confidence interval and the larger a circle, the smaller the number of observations. In order for means to be significantly different, the angle of intersection has to be less than 90°. Column C shows comparison circles that attempt to correct for a statistical Type I error (multiple comparisons) using the Tukey-Kramer test.